JOURNAL OF MATERIALS SCIENCE 19 (1984) 2980–2988

Influence of retained austenite on the fatigue endurance of carbonitrided steels

J. M. PRADO, J. L. ARQUES
Departmento de Metalurgia, Escuela Técnica Superior de Ingenieros Industriales, Barcelona, Spain

The influence of retained austenite on the rotary bending fatigue endurance of carbonitrided specimens of two different steels is investigated. Results obtained in this work support the existence of a value of retained austenite for which the fatigue limit is maximum. A model for the influence of retained austenite, based on that generally accepted for superficial residual compressive stresses, is presented. According to this model, fatigue cracks could nucleate at different sites, surface or case bottom, in specimens with austenite contents at each side of the fatigue maximum, and this maximum should occur at lower values of retained austenite in notched specimens.

1. Introduction

The existence of untransformed austenite in a great number of steels after many different thermal treatments has been known for many years [1–3]. This is an important fact, since the properties of these steels (mechanical characteristics, dimensional stability, fatigue endurance, wear resistance, etc) can be affected by the presence of different amounts of retained austenite.

The presence of retained austenite in the hardened outer layer of carburized steels is due to the decrease below room temperature of M_f, (martensite formation temperature) because of its enriched carbon content. This is more pronounced in carbonitrided steels where the presence, in relatively high amounts, of two different interstitial atoms, carbon and nitrogen, produces an even stronger decrease in the M_f temperature [4–6]. Furthermore, the presence of alloy elements and the common practice of quenching with warm oils give place to the high austenite content that can frequently be found in carbonitrided parts.

It is surprising that, in spite of its industrial relevance, no agreement has been reached on the influence which retained austenite has on the fatigue endurance in carbonitrided steels. This has been attributed to the large number of variables such as chemical composition, thermal cycle, type of atmosphere, depth of the hardened layer and others, which are involved in this thermochemical treatment [7, 8].

It is well established that the residual compressive stresses, which occur in the outer layer of steels treated in this manner, bring about an appreciable increase of the fatigue limit in rotary bending tests. The presence of retained austenite diminishes these residual stresses [9, 10] and should, therefore, have a detrimental effect on the fatigue endurance. This is the type of behaviour found by Beumelburg [10] and Razim [11]; some of their results are summarized in Fig. 1. On the other hand, certain authors, such as Tricot *et al.* [12], Wyszkowski *et al.* [13] and Schmuck [14], find a maximum for the fatigue limit around a volume fraction of 0.2 of untransformed austenite. In Fig. 2 this latter type of results are shown.

In order to try to clarify this situation we have investigated the fatigue behaviour of two different carbonitrided steels with various amounts of retained austenite. The results obtained in this work and those found in the literature are explained by means of a simple model, derived from that for superficial compressive residual stresses [15], which explains qualitatively the different types of behaviour by making clear

0022–2461/84 $03.00 + .12

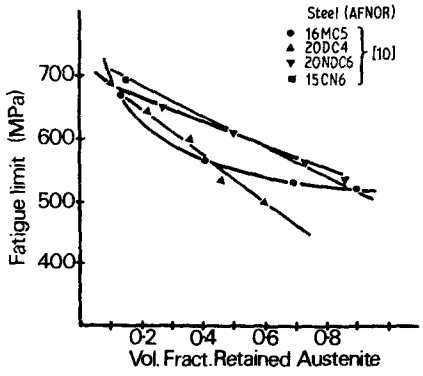

Figure 1 Variation of the rotary bending fatigue limit with retained austenite content according to Beumelburg [10].

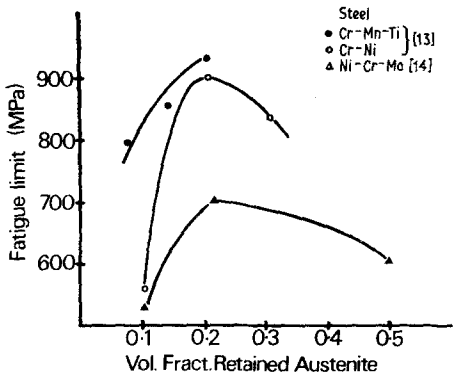

Figure 2 Variation of the rotary bending fatigue limit with retained austenite content according to Wyszkowki *et al.* [13] and Schmuck [14].

that the kind of influence exerted by austenite on fatigue is dependent on the geometry of the specimens under testing, namely whether they are notched or not.

2. Experimental procedure

The chemical composition of the two steels used in this work is shown in Table I. F-1522 (UNE designation) is a low Ni–Cr–Mo alloyed steel, while F-1540 has a higher nickel content. Both types of commercial steels were chosen because their use is widespread in the engineering design of mechanical parts undergoing rotary bending efforts.

Specimens for rotary bending fatigue tests, 96 mm gauge length and 7.52 mm diameter, were first machined and then thermochemically treated under four different compositions of furnace atmosphere, in order to obtain carbonitrided outer layers with different contents of carbon and nitrogen and thus different amounts of retained austenite. Table II gives the carbon and nitrogen contents, the carbonitrided depth and the amount of retained austenite for each combination of steel and thermal treatment. A more detailed explanation of the specimen preparation can be found elsewhere [16].

Figs. 3a and b show the hardness variation across the carbonitrided layer for each of the four families of the two steels under study. The effect of austenite is patent in treatments B, C and D for which the hardness increment with depth is due to a decreasing gradient in the austenite content. Finding a definite value for the austenite content of the hardened case, which can be used in relation with the mechanical properties of the specimens, is problematic owing to the above mentioned gradient. It is common practice to use the retained austenite content on the specimen surface, determined by X-ray diffraction, as a reference value. In our opinion it can be more meaningful to adopt as this reference value the average austenite content of the external layer, approximately 0.3 mm, where most of the austenite present in the hardened case is concentrated. This was done by ascribing an average hardness value to the external layer, derived from hardness measurements across it, and thereafter obtaining a value of the austenite content by means of the correlation between hardness and volume fraction of retained austenite established by Parrish [17]. In Fig. 4 we show the curve obtained by this author in which we have included the experimental points obtained in this work. Values extrapolated by this method were checked with optical micrographs using the etching technique developed by Klimek [18].

The high cycle fatigue limit has been determined by means of the iterative method developed by Robbins and Monro [19]. The rotary bending tests were carried out on a Shenck PUPN machine and the specimens fractures were studied by

TABLE I Chemical composition (wt %) of steels F-1522 and F-1540

Steel	C	Mn	Si	P	S	Ni	Cr	Mo
F-1522	0.23	0.80	0.29	< 0.015	0.015	0.58	0.54	0.16
F-1540	0.12	0.36	0.20	< 0.015	0.025	2.32	0.65	0.08

TABLE II Values of carbonitriding parameters

Thermal treatment	Superficial carbon content (wt %)	Superficial nitrogen (wt %)	F-1522		F-1540	
			Case depth (mm)	Volume fraction austenite	Case depth (mm)	Volume fraction austenite
A	0.523	0.490	0.90	0.09 ± 0.03	0.64	0.11 ± 0.03
B	0.948	0.133	0.97	0.18 ± 0.03	0.69	0.17 ± 0.05
C	0.840	0.550	1.05	0.38 ± 0.05	0.85	0.41 ± 0.05
D	1.060	0.300	0.80	0.46 ± 0.05	0.78	0.50 ± 0.05

scanning electron microscopy and X-ray microprobe analysis.

3. Results

3.1. Rotary bending tests

The Wöhler curves for each of the four families of the two steels under study are shown in Figs. 5a and b. We have been mainly concerned with the careful determination of the high-cycle fatigue limit, therefore the low-cycle part of the curves ($N < 10^7$) is only tentative and holds no statistical meaning. It is clear from Fig. 5 that in all cases these steels show a well-defined fatigue limit together with a marked inflexion in the Wöhler curve.

The variation of the high-cycle fatigue limit with the austenite content is shown in Fig. 6. Values obtained by others researchers, and previously presented in Fig. 2, have also been included. In all cases a maximum for the fatigue limit can be observed at austenite volume fractions close to 0.2. On the left side of these maxima (low austenite content) a unique curve can describe the behaviour of all the steels; it shows a steep increase of the fatigue limit with increasing contents of residual austenite. Values of the fatigue limit for each steel deviate from this curve at different levels, reach a maximum and then decrease with increasing amounts of austenite. Results obtained in this work for the F-1522 show a good agreement with those of Schmuck [14] for the same type of steel; discrepancy occurs only at high austenite contents and may be due to differences in its determination.

3.2. Fractography

The fracture surfaces of the specimens of the two steels under study present very similar features. The different micrographs of Fig. 7, which corresponds to steel F-1540 and thermal treatment B, show the type of fracture encountered in this work. The most outstanding feature is the occurrence of a disc-shaped crack nucleating site surrounding an inclusion lying just underneath the hardened case (Figs. 7a and b). Alumina and manganese sulphide have been found to be the most frequent types of inclusions acting as crack nucleating sites. Crack nucleation took place not by fracture of the inclusion but by decohesion of its interface with the matrix. The disc-shaped area around the inclusion shows the featureless aspect common to zones corresponding to the

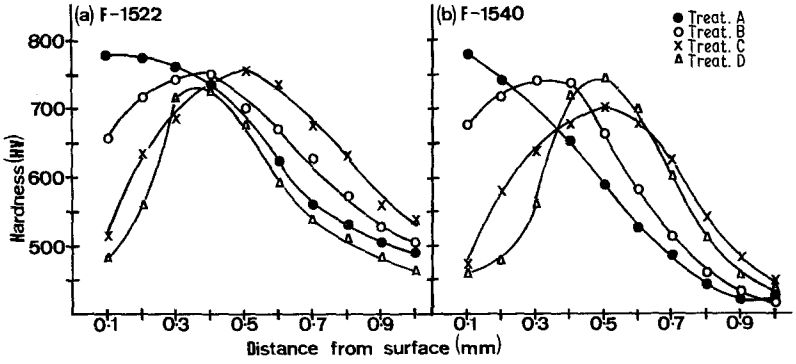

Figure 3 Hardness variation in the carbonitrided case for each of the four different thermal treatments: (a) steel F-1522; (b) steel F-1540.

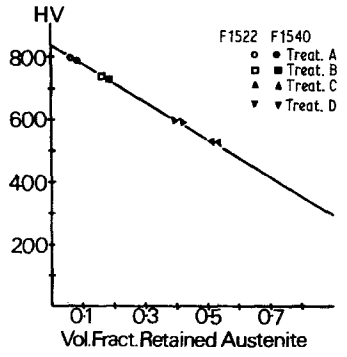

Figure 4 Variation of the superficial hardness with the amount of retained austenite in carbonitrided steels (Parrish [17]).

initial stage of a fatigue crack propagation (Fig. 7b). The crack progression towards the interior of the specimen originates the fibrous structure (Fig. 7c), characteristic of low carbon steels at relatively high crack growth rates; secondary cracks (Fig. 7d), may be seen at the bottom of what could be identified as heavily deformed striations. The different microstructure and chemical composition of the hardened case imposes a change in the mechanism of crack propagation which progressively becomes brittle intergranular (Figs. 7e and f), as the content of

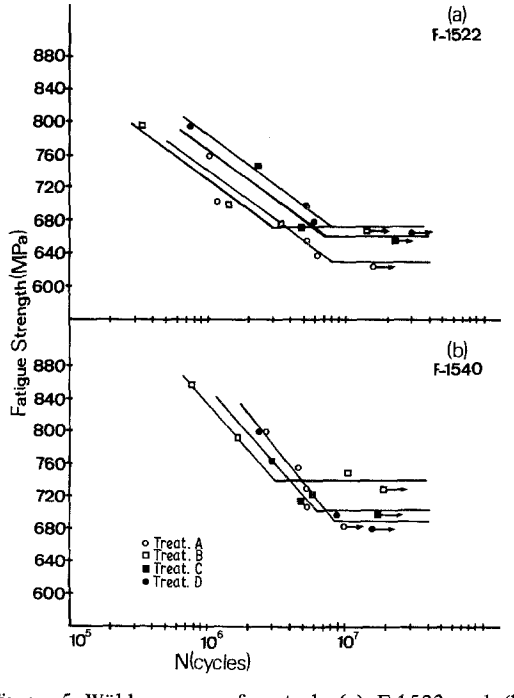

Figure 5 Wöhler curves for steels (a) F-1522 and (b) F-1540.

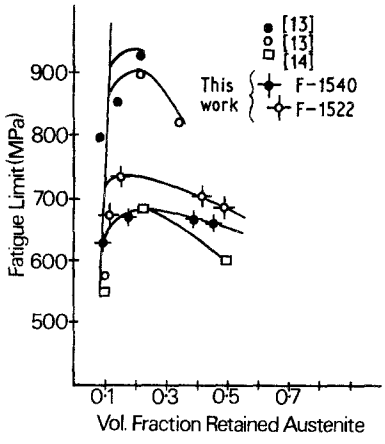

Figure 6 Variation of the fatigue limit with retained austenite content for the two steels under study. Results shown in Fig. 2 are also included.

interstitial atoms increases and consequently the amount of retained austenite. Thus, the depth of the hardened case undergoing brittle intergranular fracture was bigger in specimens with high austenite content. Finally, the area of catastrophic fracture (Fig. 7g), shows the typical dimpled structure of a ductile monotonic fracture.

The model that will be presented in the next section predicts different initial fatigue crack nucleating sites for specimens with austenite contents at each side of the maximum of Fig. 6. Low austenite specimens (volume fraction < 0.2) should nucleate their initial fatigue crack on the area just under the hardened case and obviously inclusions will be favourable sites. High austenite specimens (volume fraction > 0.2) should nucleate their initial fatigue crack on the specimen surface. The types of fractures observed in this work seem, apparently, to contradict the proposed model as for low and high austenite specimens, a crack nucleating site is always found at the case bottom. This is probably due to the fact that in high austenite specimens the inclusion surrounded by its flat disc-shaped area is only a secondary crack nucleating site and the primary one on the surface is difficult to identify as it probably lies on a grain boundary and grows by intergranular propagation. This aspect will be further discussed in the next section.

According to fracture mechanics a plastic zone should form ahead of a growing crack tip. It is also well known that martensitic transformation can take place when austenite is under plastic strain at a temperature below M_d [20].

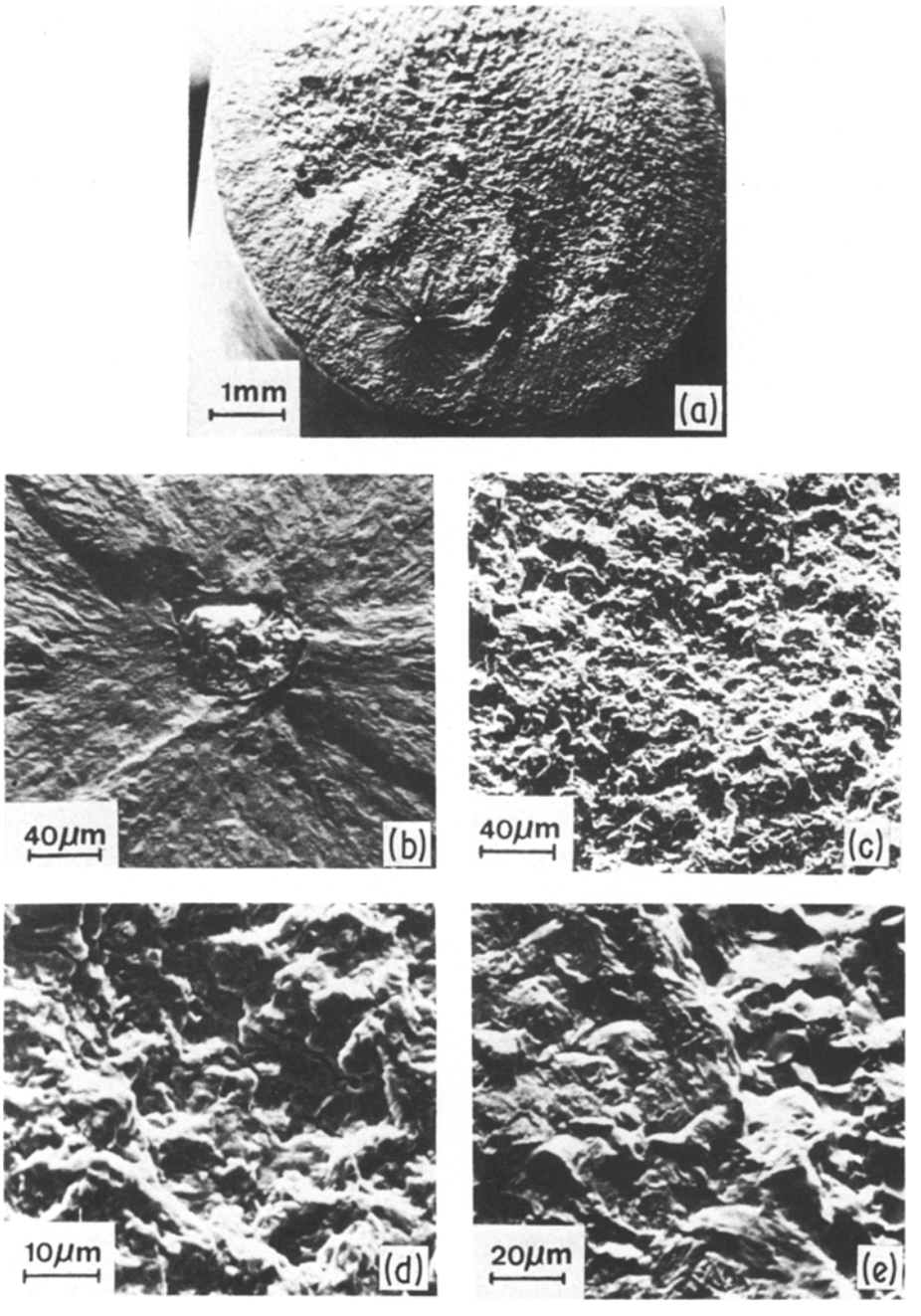

Figure 7 Scanning electron micrographs of a characteristic fracture surface corresponding to a F-1540 steel specimen with treatment B. (a) General view. (b) Crack nucleating inclusion. (c), (d) Area of fatigue crack propagation towards the specimen interior. (e), (f) Crack propagation in carbonitrided case. (g) Area of final fracture.

Thus, a fatigue crack running across a carbonitrided layer could mechanically transform the retained austenite into martensite. This is what has been observed to happen in the hardened case of F-152 and F-1540 steel specimens. The hardness variation across the carbonitrided case on a fracture surface of a F-1522 specimen (treatment B) is shown in Fig. 8; also included is the hardness curve of an untested specimen of the same steel and treatment. Hardness increases markedly in the first 0.5 mm of the case, where the retained austenite is concentrated. Beyond 0.5 mm, no

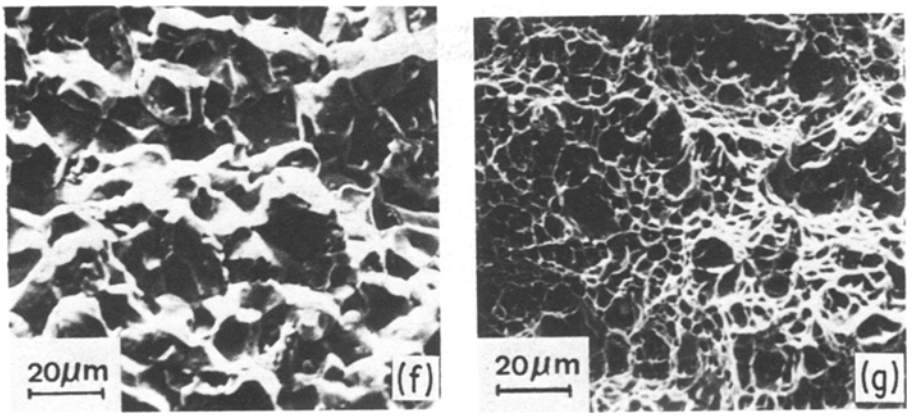

Figure 7 Continued

transformation takes place and hardness is unchanged by mechanical testing. The martensitic transformation of the retained austenite, affecting 20 μm below the crack, can be observed in the microstructures shown in Fig. 9. The effect of the propagating crack extends beyond the area of martensitic transformation which is continued by another of plastic hardening, as is shown in Fig. 10, 90 μm deep.

No evidence of martensitic transformation, in the carbonitrided case, has been detected in areas other than the one affected by the fatigue crack and described above, in contradiction with the findings of Beumelburg [10].

4. Discussion

The results which have just been reported, clearly fall into that group which finds increasing amounts of retained austenite beneficial for the fatigue limit of carbonitrided steels up to a certain value beyond which a further increase has a detrimental effect. They are apparently in contradiction with the other type of results found in the literature, for which retained austenite always has a detrimental effect. However, an important experimental difference has been detected between both groups: a different kind of specimen is used in each case. Unnotched specimens are always used in the first group, while those employed in the other group are in all cases notched [10–14]. This fact has facilitated the elaboration of a simple model which might account for both types of results.

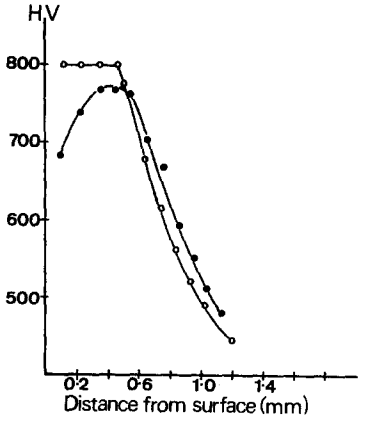

Figure 8 Hardness variation across the carbonitrided case of a fracture surface (○). Also included is the hardness variation in an untested specimen (●).

The residual stress distribution expected in a specimen with a hardened case is shown schematically in Fig. 11a [15]. Figs. 11b and c show the resulting stress distribution when an external bending stress is applied to the specimen; in this situation σ_s and σ'_s are the resulting stresses on the tensile and compressive sides of the specimen surface, and similarly σ_m and σ'_m are the resulting stresses at the case bottom. Hence in a rotary bending test the resulting stresses on the surface and case bottom will vary between σ_s and σ'_s, and between σ_m and σ'_m, respectively. The stress distribution will change when the compressive residual stress, σ_c, or the external applied stress, σ_a, vary. Therefore, in a carbonitrided steel when the retained austenite content increases, the residual compressive stress, σ_c, will decrease and consequently the stress distribution will change. A knowledge of the dependence on σ_c and σ_a of σ_s, σ'_s, σ_m and σ'_m is necessary in order to predict the influence exerted by the retained austenite on the fatigue strength. It is obvious from Fig. 11 that

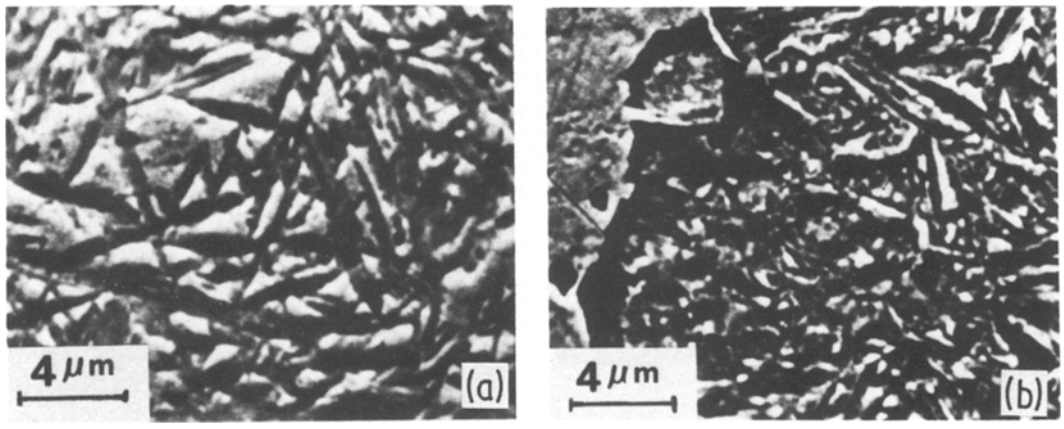

Figure 9 Scanning electron micrographs showing the martensitic transformation of the retained austenite at the fatigue crack edge. (a) Untested specimen. White areas correspond to retained austenite. (b) Fatigue crack edge.

$$\sigma_s = \sigma_a + \sigma_c$$
$$\sigma_m = \sigma_p + \sigma_n \quad (1)$$

On the other hand, from the tensional equilibrium of the residual stresses and the linear variation across the specimen section of the external applied stress, we obtain

$$\sigma_p = \frac{D-2t}{D}\,\sigma_a = K_1\sigma_a$$
$$\sigma_n = -\frac{4t(D-t)}{(D-2t)^2}\,\sigma_c = -K_2\sigma_c \quad (2)$$

Substituting Equation 2 in Equation 1, it follows that

$$\sigma_s = \sigma_a + \sigma_c$$
$$\sigma_m = K_1\sigma_a - K_2\sigma_c \quad (3)$$

where K_1 and K_2 are geometrical factors depending on specimen diameter, D, and case thickness t. Similar equations can be derived for σ'_s and σ'_m; The variation of σ_s, σ'_s, σ_m and σ'_m with the residual compressive stress σ_c, for a set of experimental values of σ_a, D and t, is shown in Fig. 12. The following consequences can be derived from Equation 3 and Fig. 12;

1. The peak tensile value, σ_m, of the cyclic stress on the specimen case bottom decreases with decreasing residual compressive stress, σ_c, or in other words, with increasing retained austenite;

2. The peak tensile value, σ_s, of the cyclic stress on the specimen surface increases with decreasing residual compressive stress, σ_c, and therefore with increasing retained austenite;

3. There is a value, $\sigma_{c,0}$ of the residual compressive stress such that;

$$\sigma_m = \sigma_s \text{ for } \sigma_c = \sigma_{c,0}$$
$$\sigma_m > \sigma_s \text{ for } |\sigma_c| > |\sigma_{c,0}|$$
$$\sigma_m < \sigma_s \text{ for } |\sigma_c| < |\sigma_{c,0}| \quad (4)$$

Hence, when $|\sigma_c| > |\sigma_{c,0}|$, low retained austenite content, the maximum tensile value of the cyclic stress occurs at the case bottom and it is here that the initial fatigue crack should nucleate. According to point 1, the specimen fatigue endurance should increase with decreasing residual compressive stress, namely with increasing retained austenite content.

When $|\sigma_c| < |\sigma_{c,0}|$, high retained austenite content, the maximum tensile value of the cyclic stress is no longer at the case bottom but on the specimen surface, and consequently this should be the preferential fatigue crack nucleating site. Now, and according to point 2, the specimen fatigue endurance should decreases with decreasing

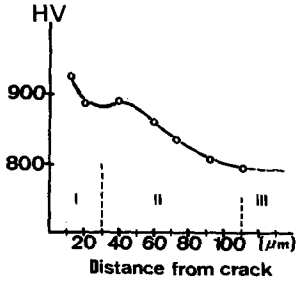

Figure 10 Hardness variation with distance from fatigue crack. Zone I area of martensitic transformation Zone II area of strain hardening. Zone III unaffected area.

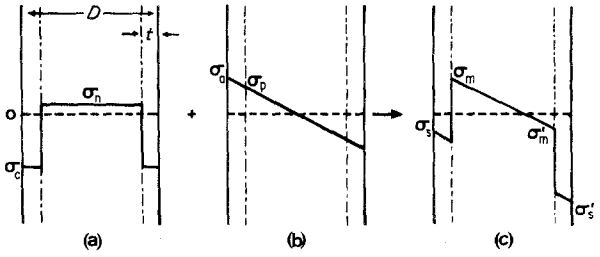

Figure 11 Schematic representation of stress distribution in a carbonitrided cylindrical specimen under bending condition. (a) Residual stress distribution. (b) Applied external stress. (c) Resultant stress distribution.

residual compressive stress or increasing retained austenite content.

Thus, it is obvious that the specimen fatigue endurance will reach a maximum for a retained austenite content such that $\sigma_c = \sigma_{c,0}$. According to our experimental results, this fatigue maximum occurs at a relatively low austenite content, close to 0.2, while the model presented here predicts this maximum for a small residual compressive stress of the order of 100 MPa. This results seems to indicate a strong initial dependence of σ_c on austenite content, becoming progressively weaker as the austenite content increases. Not much work has been carried out in this field, but results from Beumelburg [10] and Diament *et al.* [9] show this type of behaviour.

Finally, the case of notched specimens should be considered. The stress concentration at the root of the notch will change the resultant stress distribution and, in particular, σ_s will become

$$\sigma_s = K_t(\sigma_a + \sigma_c) \qquad (5)$$

where K_t is the stress concentration factor.

The shift to the left of the σ_s line, shown in Fig. 13 for $K_t = 2$ and $K_t = 3$, will produce a similar shift of the fatigue limit towards lower retained austenite contents. Considering the experimental difficulty of producing carbonitrided layers with volume fractions of austenite below 0.1 it is not surprising that a maximum for the fatigue limit of carbonitrided notched specimens has not been detected. From our point of view, the fact that notched specimens quenched below room temperature show a strong decrease of the fatigue limit, can be due not only to the possible damage done to the case by microcracks during the cooling as it has been proposed by Beumelburg [10], but to a change in the austenite content across the fatigue maximum as the model proposed in this paper predicts.

For further verification of the model proposed above, fatigue tests were carried out on specimens of F-1540 steel and treatment A, so that they should initiate their fatigue failure on the case bottom. A superficial notch effect was produced by means of a Rockwell 30N hardness mark. All the fractures nucleated on the specimens surface, with no sign of crack nucleation on the case bottom, corresponding with the predictions of Fig. 13. Evidently, this type of behaviour,

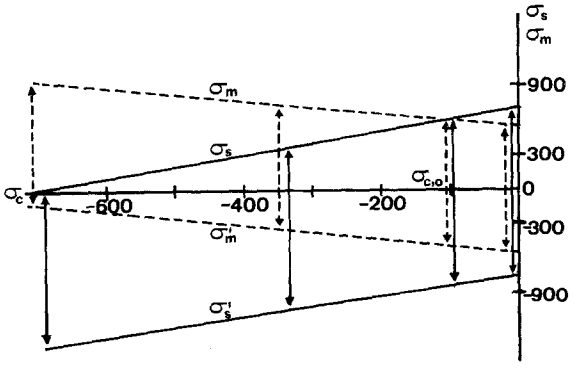

Figure 12 Variation of superficial and case bottom stresses σ_s, σ'_s, σ_m, σ'_m, with residual compressive stress, σ_c, in the carbonitrided case according to Equation 3. Experimental values are, $D = 7.52$ mm, $t = 0.80$ mm and $\sigma_a = 700$ MPa. (Units of both axes are in MPa.)

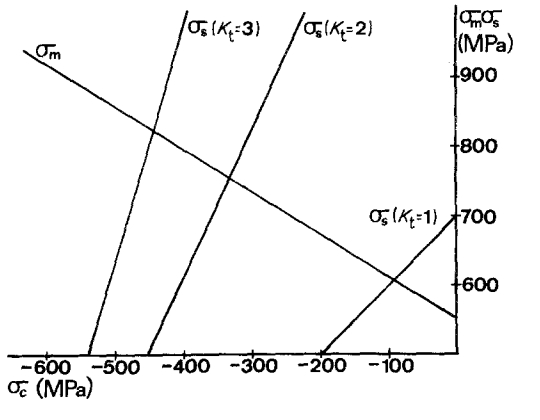

Figure 13 Effect in notched specimens of different values of stress concentration factor, K_t, on the variation of the superficial resultant stress, σ_s, with austenite content, σ_c.

previously not clearly observed in the case of unnotched specimens with high austenite content, is due to the pronounced difference between the stresses acting on the surface and the case bottom which makes secondary crack nucleation highly improbable. This stress difference is much smaller in the case of unnotched specimens (Figs. 12 and 13); therefore, secondary crack nucleation could now take place. In conclusion, the transition from case bottom fatigue crack nucleation in specimens with low austenite content to surface nucleation in specimens with high austenite content is not abrupt, but there is a span of intermediate retained austenite contents for which fatigue crack nucleation can occur simultaneously on both sites. This retained austenite span narrows and shifts towards lower austenite contents in notched specimens.

5. Conclusions

As the result of this work the following main conclusions may be derived:

1. There is always an optimum austenite content for which the rotary bending fatigue endurance of carbonitrided steels reaches a maximum;

2. The optimum volume fraction of retained austenite lies between 0.2 and 0.3 in unnotched specimens and shifts to lower values in notched specimens;

3. The model usually applied for superficial compressive residual stresses explains satisfactorily the different kinds of behaviour found in the fatigue endurance of carbonitrided steel parts.

It can be concluded, from a practical point of view, that in parts with mild geometrical stress raisers austenite volume fractions up to 0.2 or 0.3 will have a beneficial effect on their rotary bending fatigue resistance, but it should be kept to between 0.1 and 0.2 in those parts with strong geometrical stress raisers. Retained austenite volume fractions below 0.1 should be prevented in all cases.

References

1. M. COHEN, *Trans. ASM* **41** (1949) 35.
2. A. CONSTANT and G. MURRAY, *Rev. Metal.* November (1970) 899.
3. Y. MEYZAUD and C. SAUZAY, *Trait Therm.* **81** (1974) 33.
4. I. S. I., "Heat Treatment of Engineering Components" (Lund Humphrey, London, 1970) p. 125.
5. B. J. FERNANDEZ, F. MEDINA and J. M. BELLO, *Rev. Metal. (CENIM)* **9** (1973) 181.
6. M. L. GRINBERG and A. L. BUGOSLONSKY, *Metallov. Term. Obrabot.* 8 (1969) 60.
7. J. L. ARQUES, *Dyna* **2** (1978) 43.
8. K. FUNATANI, *Trait. Therm.* **63** (1972) 41.
9. A. DIAMENT, R. AL HAIK, R. LAFONT and R. WYSS, *ibid.* 87 (1974) 87.
10. W. BEUMELBURG, *ibid.* **98** (1975) 39.
11. C. RAZIM, *Härterei-techn Mitt.* **23** (1968) 1.
12. R. TRICOT, M. LACOUDE and B. CHAMPIN, *Rev. Metal.* July/August (1972) 497.
13. J. WYSZKOWKI, H. PRIEGNITZ, A. RATKIEWICKZ and E. GOZDZIK, *ibid.* June (1971) 411.
14. J. SCHMUCK, *Aciers Speciaux* **33** (1976) 5.
15. G. E. DIETER, "Mechanical Metallurgy" (McGraw-Hill, New York, 1976) p. 431.
16. J. L. ARQUES, PhD thesis, Escuela Tecnica Superior Ingenieros Industriales, Barcelona (1982).
17. G. PARRISH, *Heat Treat. Metals* **4** (1976) 101.
18. E. J. KLIMEK, *Trait. Therm.* **99** (1975) 41.
19. H. ROBBINS and S. MONRO, *Annals Math. Statistics* **22** (1951) 400.
20. J. D. VERHOEVEN, "Fundamentals of Physical Metallurgy" (John Wiley, London, 1975) p. 496.

Received 2 August
and accepted 29 November 1983